AIP | Applied Physics Letters

Real-time in situ spectroscopic ellipsometry of GaSb nanostructures during sputtering

I. S. Nerbø, S. Le Roy, M. Kildemo, and E. Søndergård

Citation: Appl. Phys. Lett. **94**, 213105 (2009); doi: 10.1063/1.3133350
View online: http://dx.doi.org/10.1063/1.3133350
View Table of Contents: http://apl.aip.org/resource/1/APPLAB/v94/i21
Published by the American Institute of Physics.

Real-time *in situ* spectroscopic ellipsometry of GaSb nanostructures during sputtering

I. S. Nerbø,[1,a)] S. Le Roy,[2] M. Kildemo,[1] and E. Søndergård[2]
[1]*Department of Physics, Norwegian University of Science and Technology (NTNU), NO-7491 Trondheim, Norway*
[2]*UMR 125 Unité mixte CNRS/Saint-Gobain Laboratoire Surface du Verre et Interfaces, 39 Quai Lucien Lefranc, F-93303 Aubervilliers Cedex, France*

(Received 23 February 2009; accepted 21 April 2009; published online 27 May 2009)

We demonstrate that real-time *in situ* spectroscopic ellipsometry can be used to measure the height evolution of nanostructures during low energy ion sputtering of GaSb. A graded anisotropic effective medium approximation is used to extract the height from the optical measurements. Two different growth regimes have been observed, first exponential then followed by a linear regime. The linear regime is not expected from the traditional sputtering theories. The *in situ* results correspond well to *ex situ* atomic force microscopy measurements. © *2009 American Institute of Physics*. [DOI: 10.1063/1.3133350]

Self-organized nanostructures open for efficient and low-cost production of materials with new and interesting properties, with potential applications in electronics, optics, and life sciences.[1–4] A major challenge for controlling and understanding growth processes for such structures is the characterization of nanometer sized features. Traditional near field techniques, such as atomic force microscopy (AFM), scanning electron microscopy, and transmission electron microscopy, are time consuming and not suited for *in situ* use. A fast observation technique compatible with vacuum chambers is necessary for studies of growth laws and their dependence on formation conditions. Grazing-incidence small-angle x-ray scattering (GISAXS) has been used for real time *in situ* characterization of nanostructures during growth, with subnanometer sensitivity.[5,6] Unfortunately, this technique requires an intense well-collimated x-ray beam, typically provided by a synchrotron. Spectroscopic ellipsometry (SE) is on the other hand a much more accessible alternative, based on measuring the change of polarization state of light, and ellipsometers can easily be mounted on most growth chambers. It is a much used technique for accurately measuring dielectric functions and the thickness of thin layers (see e.g., Ref. 7), and for real-time monitoring of thin film growth (see e.g., Refs. 8–10). In this work we demonstrate the capability of SE to monitor the height evolution of nanostructures from real-time *in situ* measurements. As an example of nanostructuration, we have studied low energy ion sputtering of GaSb, leading to high aspect ratio pillars. Such structures have interesting antireflective properties[11] and have recently been reported to have a formation process induced by nanoscale segregation of Ga,[12] which could have interesting implications for the growth law.

The nanostructures were prepared on commercially available GaSb(100) wafers, in an ultrahigh vacuum chamber with a base pressure of 10^{-8} mbar. The sputter gas was 300 eV Ar+ with a flux of (0.017 ± 0.001) mA/scm^2. The ion incidence was normal to the sample surface, and all samples were sputtered at room temperature. A SE (MM16, Horiba Jobin Yvon) with a fast charged-coupled device (CCD) based spectrograph (spectral range 1.46–2.88 eV) was used to do *in situ* measurements during sputtering. A sketch of the setup is shown in Fig. 1.

A series of samples have been observed *in situ* for different exposure times to the ion beam, ranging from 2 to 30 min. After sputtering the surfaces were characterized by AFM. Figure 2 shows an image of a sample surface after sputtering, revealing disordered nanopillars with regular shape and size, which can be described as truncated cones (see inset of Fig. 2).

In situ SE spectra were recorded every fifth second during the sputtering, by measuring the ellipsometric intensities I_S and I_C. Samples sputtered under normal ion incidence gives no polarization coupling,[11,13] in this case the latter can be expressed as $I_S = \sin 2\Psi \sin \Delta$ and $I_C = \sin 2\Psi \cos \Delta$, where Ψ and Δ are defined from the ratio of the complex reflection coefficients $r_{pp}/r_{ss} = \tan \Psi \exp(i\Delta)$. Examples of SE measurements at different stages in the sputtering process are presented in Fig. 3. The surface structure has a strong impact on the optical response, indicating that SE is highly sensitive to such features.

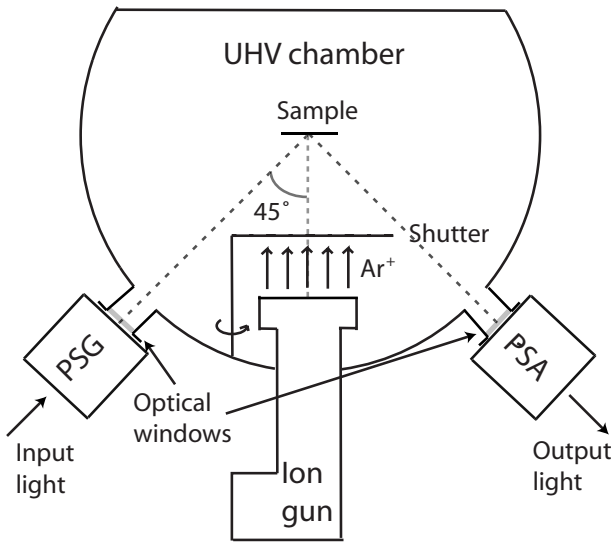

FIG. 1. Sketch of the experimental setup. The polarization state generator (PSG) and the polarization state analyzer (PSA) of the ellipsometer were mounted on two low-strain optical windows, giving a fixed angle of incidence of 45° on the sample.

a)Electronic mail: ingar.nerbo@ntnu.no.

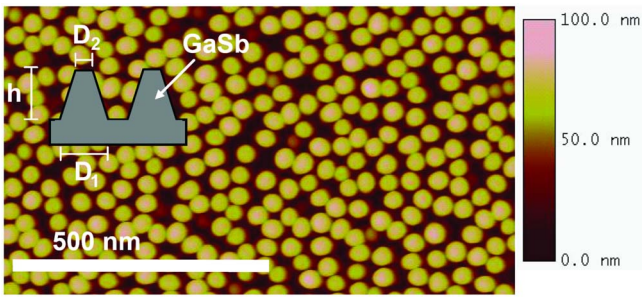

FIG. 2. (Color online) AFM image of the sample sputtered for 30 min. The inset is a sketch of the optical model, where h is the total height of the pillars and D_1 and D_2 are the bottom and top relative diameters.

In a previous publication we demonstrated that the height of such nanostructures can be found by *ex situ* ellipsometry,[11] through effective medium modeling of the optical properties. The same model have been used to simulate the *in situ* SE measurements, simplified by neglecting the oxide coating since the samples are measured in vacuum. The effective medium approximation is valid as long as the lateral dimension of the structures are sufficiently smaller than the wavelength of light. The effective dielectric function is calculated by treating the pillars as a stack of cylinders of GaSb with decreasing radius, surrounded by void. The effective dielectric function for each layer is found by using a generalized Bruggeman effective medium equation for ellipsoidal inclusions,[14]

$$f_{\mathrm{GaSb}}\frac{\epsilon_{\mathrm{GaSb}}-\epsilon_{\mathrm{ii}}}{\epsilon_{\mathrm{ii}}+L_i(\epsilon_{\mathrm{GaSb}}-\epsilon_{\mathrm{ii}})}+f_v\frac{\epsilon_v-\epsilon_{\mathrm{ii}}}{\epsilon_{\mathrm{ii}}+L_i(\epsilon_v-\epsilon_{\mathrm{ii}})}=0, \qquad (1)$$

where f and ϵ denote the filling factors and complex dielectric functions, respectively, with the subscript GaSb referring to the crystalline core, and v to the surrounding void. L_i denotes the depolarization factor in direction i (along a principal axis of the structure) and ϵ_{ii} is the effective dielectric function in direction i. For cylindrical inclusions, $L_{\parallel}=0.5$ parallel to the mean surface, and $L_{\perp}=0$ perpendicular to the mean surface. This gives a uniaxial anisotropic material with the optic axis normal to the mean surface. In this case there is no polarization coupling ($r_{\mathrm{ps}}=r_{\mathrm{sp}}=0$). Reflection coefficients for a stack of anisotropic layers have been calculated by an implementation of Schubert's algorithm,[15] based on Berreman's 4×4 differential matrices.[16]

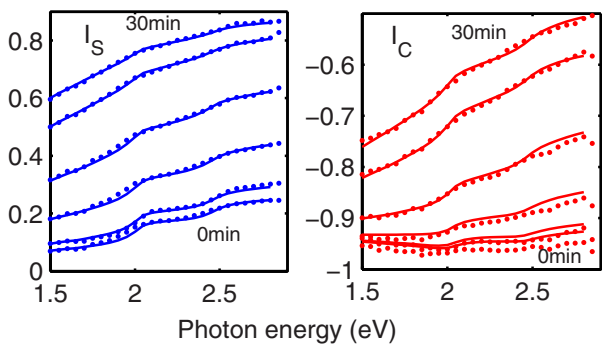

FIG. 3. (Color online) *In situ* SE measurements (dots) of a sample at different stages in the formation process [after 0 (bottom curves), 1, 2, 3, 10, and 30 (top curves) minutes of sputtering], together with fitted effective medium models (solid lines).

TABLE I. Comparison between *in situ* SE results and *ex situ* AFM measurements. h_{SE} and h_{AFM} are the heights found from SE and AFM and K_{AFM} is the mean nearest neighbor distance as estimated from AFM.

Time	100 s	2 min	3 min	5 min	10 min	30 min
h_{SE}(nm)	19	27	38	48	57	83
h_{AFM}(nm)	22	26	35	46	55	82
K_{AFM}(nm)	39	41	43	41	45	51

Three parameters in the model have been fitted to the experimental measurements by minimizing a χ^2 function, as reported in Ref. 11. These parameters are the total height h of all layers, and the relative effective diameters D_1 and D_2 of the bottom and top cylinder, respectively (see inset of Fig. 2). The diameters of the cylinders in intermediate layers decrease linearly from D_1 to D_2. The diameters have been normalized to the nearest neighbor distance, since only volume filling factors affect the effective medium. The absolute lateral size of the structures cannot be found from SE when the effective medium approximation is valid. The filling factors have been calculated for hexagonal ordering, to model a random structure with on average six nearest neighbors.[11]

The height inferred from the *in situ* SE measurements are compared to AFM height measurements in Table I, together with the lateral dimensions found by AFM. The two heights are in good correspondence for all the samples. From Monte Carlo simulations and the observed noise level, the dynamical sensitivity of the height derived from SE has been estimated to be less than 1 nm. Finding the mean height of this kind of densely packed high-aspect ratio structures from AFM measurements is challenging, as images of these surfaces are very sensitive to tip effects. The tip may not always reach the bottom between closely packed pillars, and to account for this the height of each top have been calculated in relation to a local minimum within a certain distance (d) from the top. The mean height calculated this way increases strongly with d as the distance is shorter than the mean bottom pillar radius. Then it saturates, and the mean height found then is a good approximation to the real mean pillar height. This saturation distance corresponds well to half the mean nearest neighbor separation as estimated by AFM.

The height evolution of the samples during sputtering is derived from the SE measurements, and presented in Fig. 4. The evolution of the different samples is observed to be very reproducible. Initially the GaSb wafers are covered by an approximately 7 nm thick oxide layer, which will be removed at the initial stage of sputtering. In this stage the effective medium model described above is not valid, but still shows a decrease in height, corresponding to removal of oxide and possibly smoothing of the surface. After about 1 min the height of the structure starts to increase at an exponential rate of 0.0225 s^{-1}, lasting about 1 min. The growth is then followed by a transition stage, until it becomes clearly linear after approximately 6 or 7 min of sputtering, with a growth rate of 0.019 nm/s. No height saturation is observed within 30 min. The average deviation from a linear fit for the last 15 min of sputtering is 0.3 nm. The mean nearest neighbor distance estimated from the AFM measurements seems to be unchanged for the first 5 min of sputtering, and then to increase slowly after the transition to linear growth, with a total increase of approximately 10 nm after 30 min.

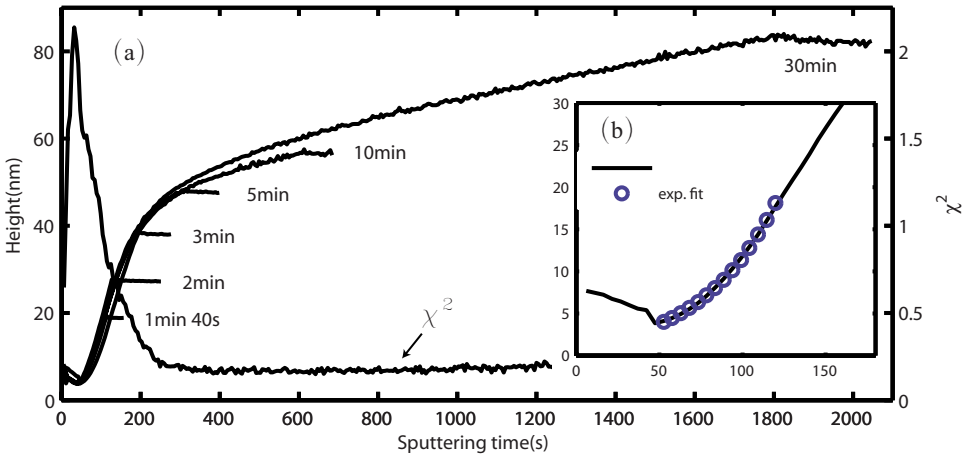

FIG. 4. (Color online) (a) Height evolution of GaSb nanopillars during low energy ion sputtering, for various ion beam exposure times, together with the χ^2 error function for the sample sputtered 30 min. (b) Initial growth stage of the sample sputtered for 30 min.

The initial exponential growth of the height during sputtering can be explained by Bradly and Harper's (BH) theory,[17] where the growth is due to the competition between the curvature dependent sputtering yield[18] and diffusion processes. Nonlinear extensions of the BH model have been performed to describe the formation of nanostructured GaSb,[19,20] but the observed linear regime has neither been observed nor predicted. Le Roy *et al.*[12] have ascribed the pillar growth to gallium segregation. Gallium rich zones will act as a sputter shield, and could account for the linear regime.

SE combined with appropriate modeling proves to be a sensitive tool for *in situ* characterization of the formation of nanostructures. In principle, this method gives results comparable to GISAXS synchrotron measurements for the amplitude of the structures. Real-time height evolution can be accurately determined from SE and effective medium models. Information on lateral dimensions on the nanoscale cannot be found from SE measurements in the visible range, while it can be obtained with GISAXS.[6] However, a major advantage is that SE is a table top setup that can easily be adapted to most growth chambers. The method has given new insight in the formation process of GaSb nanopillars. It opens for an effective way to study the dependence of the formation process on physical parameters such as temperature, ion flux, and energy. Such studies would be time consuming and less accurate if performed by standard imaging tools.

We are thankful to Horiba Jobin Yvon for help with adapting the ellipsometer for *in situ* use. We acknowledge support from the Aurora mobility program. In addition, S.L.R. and E.S. acknowledge support from the ANRT and Saint-Gobain.

[1] L. Samuelson, Mater. Today **6**, 22 (2003).
[2] W. Wu, Appl. Phys. Lett. **90**, 063107 (2007).
[3] A. Lafuma and D. Quéré, Nature Mater. **2**, 457 (2003).
[4] S. J. Wilson and M. C. Hutly, Opt. Acta **29**, 993 (1982).
[5] G. Renaud, R. Lazzari, C. Revenant, A. Barbier, M. Noblet, O. Ulrich, F. Leroy, J. Jupille, Y. Borensztein, C. R. Henry, J.-P. Deville, F. Scheurer, J. Mane-Mane, and O. Fruchart, Science **300**, 1416 (2003).
[6] O. Plantevin, R. Gago, L. Vázquez, A. Biermanns, and T. H. Metzger, Appl. Phys. Lett. **91**, 113105 (2007).
[7] R. M. A. Azzam and N. M. Bashara, *Ellipsometry and Polarized Light* (North-Holland, Amsterdam, 1987).
[8] W. M. Duncan and S. A. Henck, Appl. Surf. Sci. **63**, 9 (1993).
[9] R. W. Collins, I. An, H. Fujiwara, J. Lee, Y. Lu, J. Koh, and P. I. Rovira, Thin Solid Films **313**, 18 (1998).
[10] M. Kildemo, R. Brenot, and B. Drévillon, Appl. Opt. **37**, 5145 (1998).
[11] I. S. Nerbø, M. Kildemo, S. Le Roy, I. Simonsen, E. Søndergård, L. Holt, and J. Walmsley, Appl. Opt. **47**, 5130 (2008).
[12] S. Le Roy, N. Brun, A. Lelarge, E. Søndergård, and E. Barthel, "Self-sustained etch masking is at the origin of the formation of nanopillars during ion erosion of III-V semiconductors" (unpublished).
[13] M. Kildemo, I. S. Nerbø, E. Søndergård, L. Holt, I. Simonsen, and M. Stachakovsky, Phys. Status Solidi C **5**, 1382 (2008).
[14] J. E. Spanier and I. P. Herman, Phys. Rev. B **61**, 10437 (2000).
[15] M. Schubert, Phys. Rev. B **53**, 4265 (1996).
[16] D. W. Berreman, J. Opt. Soc. Am. **62**, 502 (1972).
[17] R. M. Bradley and J. M. E. Harper, J. Vac. Sci. Technol. A **6**, 2390 (1988).
[18] P. Sigmund, Phys. Rev. **184**, 383 (1969).
[19] M. Castro, R. Cuerno, L. Vázquez, and R. Gago, Phys. Rev. Lett. **94**, 016102 (2005).
[20] S. Facsko, T. Dekorsy, C. Koerdt, C. Trappe, H. Kurz, A. Vogt, and H. L. Hartnagel, Science **285**, 1551 (1999).